

# Constraining the central engine of radio-loud AGNs

Rita M. Sambruna<sup>a</sup>, Michael Eracleous<sup>a</sup>,  
Richard F. Mushotzky<sup>b</sup>

<sup>a</sup>*Department of Astronomy and Astrophysics, The Pennsylvania State University,  
525 Davey Lab, State College, PA 16802*

<sup>b</sup>*NASA/GSFC, Code 662, Greenbelt, MD 20771*

---

## Abstract

We present an X-ray spectral survey of radio-loud (RL) AGNs using *ASCA* and *RXTE*. The goal was to study the structure of their central engines and compare it to that of their radio-quiet (RQ) counterparts. We find systematic differences in the X-ray properties of the two AGN classes. Specifically, RL AGNs exhibit weaker Fe lines and reflection components than RQ AGNs, indicating smaller solid angles subtended by the reprocessing medium to the X-ray source. The circumnuclear environs of RL and RQ AGNs also differ: large amounts of cold gas are detected in Broad Line Radio Galaxies and Quasars, contrary to what is found in Seyfert galaxies of similar X-ray luminosity. We also discuss *ASCA* observations of Weak Line Radio Galaxies, a distinct subset of radio galaxies which may harbor a low-luminosity AGN powered by an advection-dominated accretion flow.

*Key words:* Radiogalaxies; X-rays; black hole; AGNs.

---

## 1 Introduction

One of the fundamental open questions in our understanding of Active Galactic Nuclei (AGN) is the difference between radio-loud (RL)<sup>1</sup> and radio-quiet (RQ) objects. In the current AGN paradigm, their power is ultimately provided by accretion of gas from the host galaxy onto a central black hole. While this picture holds for both RQ and RL objects (Urry & Padovani 1995, Antonucci 1993), it is intriguing that the latter are able to produce powerful, collimated relativistic jets which instead are weak or absent in their RQ

---

<sup>1</sup> We exclude blazars, whose radiation properties are dominated by beamed emission from the jet.

counterparts. While the environments of RL and RQ objects are different, as are the host galaxies (RL AGNs are found exclusively in elliptical galaxies), exactly how these large scale phenomena influence the nature of the central engine is unknown. More intrinsic physical differences related to the properties of the accretion flow or the central black hole is also a candidate cause of the dichotomy between RL and RQ AGNs. In particular, RL AGNs may harbor rapidly spinning black holes (Blandford & Znajek 1977, Meier 1999) and/or very large accretion disks (Blandford & Payne 1982), or their inner disks may have the form of an advection-dominated (ion) torus (Rees et al. 1982, Narayan & Yi 1994, Narayan & Yi 1995).

The X-ray spectra of AGNs may be the means by which we understand the difference between RL and RQ sources since the X-ray emission is associated with the hottest, innermost parts of the accretion flow. Indeed, models for jet formations predict different accretion structures and thus different X-ray radiation properties. It is therefore encouraging that a number of systematic differences exist between the X-ray continua of RL and RQ AGNs from earlier *Einstein* and *EXOSAT* data (Wilkes & Elvis 1987, Lawson et al. 1992), with RL AGN having somewhat flatter X-ray spectra and higher X-ray luminosities than RQ ones.

The advent of *ASCA*, with its improved spectral resolution, and of *RXTE*, with its wide energy coverage and large collecting area, has opened a new chapter in the study of the X-ray properties of AGN. *ASCA* observations of Seyfert 1s established that these objects exhibit a strong (Equivalent Width  $EW \sim 250$  eV) and broad (FWHM  $\sim 50,000$  km/s) fluorescent Fe  $K\alpha$  line at 6.4 keV (rest-frame), with an asymmetric red wing (Nandra et al. 1997). The line profiles are consistent with an origin from the inner parts of an accretion disk (Fabian et al. 1989). At higher energies, Seyfert 1s exhibit a “bump” in their spectra peaking around 20–30 keV (Nandra & Pounds 1994, Weaver et al. 1998), which is attributed to Compton reflection of the primary, power-law continuum from a cold reprocessor, most likely the accretion disk (George & Fabian 1991).

Soft X-ray observations of AGNs can also probe the immediate black hole environment. In 50% of the Seyfert 1s observed with *ASCA*, evidence for absorption features around 0.6–0.7 keV (the range of ionized oxygen) were observed (George et al. 1998, Reynolds 1997). This indicates the presence of a “warm absorber” along the line of sight to the nucleus in these systems, with densities  $N_H^W \sim 10^{21-24} \text{ cm}^{-2}$ .

In order to study the structure of their central engines, we undertook a systematic spectral survey of RL AGN using public *ASCA* data as well as new observations with both *ASCA* and *RXTE*. More details can be found in Sambruna, Eracleous, & Mushotzky (1999) and Eracleous, Sambruna, & Mushotzky (1999),

together with references to previously published works.

## 2 The ASCA and RXTE samples

The *ASCA* sample includes all lobe-dominated radio-loud AGN with public data up to September 1998. A subdivision was performed on the basis of the optical spectroscopic properties (Sambruna, Eracleous, & Mushotzky 1999), such as the presence of broad, permitted lines in their optical spectra and the luminosity of the [O III]  $\lambda 5007$  line. The final sample, which is not unbiased or statistically complete by any means, includes 9 Broad Line Radio Galaxies (BLRGs), 6 Quasars, (QSRs), 12 Narrow Line Radio Galaxies (NLRGs), and 11 Radio Galaxies (RGs), of mixed FR I and FR II types. The sample objects have redshifts  $z \lesssim 0.5$ .

The *RXTE* sample (Eracleous, Sambruna, & Mushotzky 1999) contains four nearby, X-ray bright BLRGs ( $F_{2-10 \text{ keV}} \sim 1 - 4 \times 10^{-11} \text{ erg s}^{-1}$ ). Of these, 3C 120 and 3C 111 are superluminal sources and the inclination of the jet with respect to the observer is constrained from radio observations (Eracleous & Halpern 1998); lower limits on the jet inclination are obtained for the other two BLRGs, 3C 382 and Pictor A, from their large scale radio morphology.

## 3 Results

A power-law spectral component in the 2–10 keV band, most likely coming from the AGN, is detected by *ASCA* in 90% of the sources. The average photon index is  $\langle \Gamma_X \rangle \sim 1.7 - 1.9$  for all the four subclasses (in agreement with unification models). Similar slopes are found with *RXTE* for the four observed BLRGs. The distribution of  $\Gamma_X$  among BLRGs, QSRs, NLRGs, and RGs is not demonstrably different from RQ AGNs of matching intrinsic X-ray luminosity. Thus, our results support previous claims that the flatter spectra of RL AGNs are a result of a contribution from a beamed component from the jet. This conclusion is bolstered by the fact that no correlation between the nuclear X-ray luminosity and the core radio luminosity is observed for our sample of (lobe-dominated) RL sources.

At soft energies ( $< 2 \text{ keV}$ ), we find no evidence for ionized absorption in the BLRGs of our sample (with the exception of 3C390.3), in striking contrast to Seyfert 1s. Instead, we detect large columns of *cold* gas. Figure 1a shows the histogram of the *excess* X-ray column density  $N_{\text{H}}^{\text{exc}}$  (defined as the difference between the fitted X-ray column and the Galactic value in the direction to the source) for the four classes of RL AGNs. Large columns,  $N_{\text{H}}^{\text{exc}} \sim 10^{21-24}$

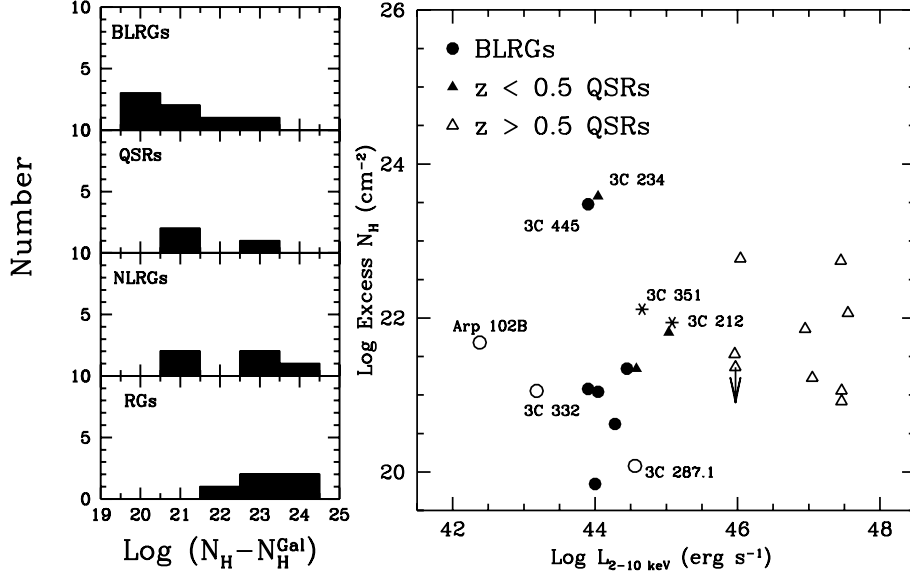


Fig. 1. (a) Left: Histogram of the excess X-ray absorption, defined as the difference between the fitted  $N_H$  with *ASCA* and the Galactic value, including SIS systematic effects. A fraction of BLRGs and QSRs, plotted here, have column densities of cold gas similar to NLRGs and RGs. (b) Right: Plot of the intrinsic (rest-frame) excess  $N_H$  versus luminosity for the BLRGs and QSRs of our study, together with more distant sources studied with *ROSAT* and *ASCA* in the literature. No trends of the column density with luminosity are apparent over more than five decades.

$\text{cm}^{-2}$ , are measured in type 2 objects (NLRGs and RGs), presumably due to the obscuring torus (Urry & Padovani 1995). What is more puzzling is the detection of similar columns in a fraction ( $\sim 44\text{--}60\%$ ) of BLRGs and QSRs, where according to the unified schemes the line of sight to the nucleus should be devoid of cold gas.

The excess X-ray columns in the BLRGs and QSRs of our sample are similar to those observed in more distant RL objects with *ASCA* and *ROSAT* (Elvis et al. 1998, Cappi et al. 1997). This is apparent from Figure 1b, where the intrinsic  $N_H^{\text{exc}}$  (in the source's rest-frame) is plotted versus the nuclear 2–10 keV luminosity. While there is a large dispersion in the values of the column density at lower luminosity, there are no trends over more than five decades: the more distant sources have similar intrinsic absorbing columns to the nearby sources. The origin of the absorbing medium and its location are not known. However, it is interesting to note that the more distant objects are mostly core-dominated QSRs, contrary to our sources, possibly implying an isotropic distribution of the absorber around the X-ray source. Future high-resolution observations with *Chandra* and XMM will help clarify the nature of the X-ray absorber.

The Fe  $K\alpha$  line is detected by *ASCA* in 67% of BLRGs, 20% of QSRs, 33% of NLRGs, and 30% of RGs. In BLRGs and QSRs the line is broad, with FWHM

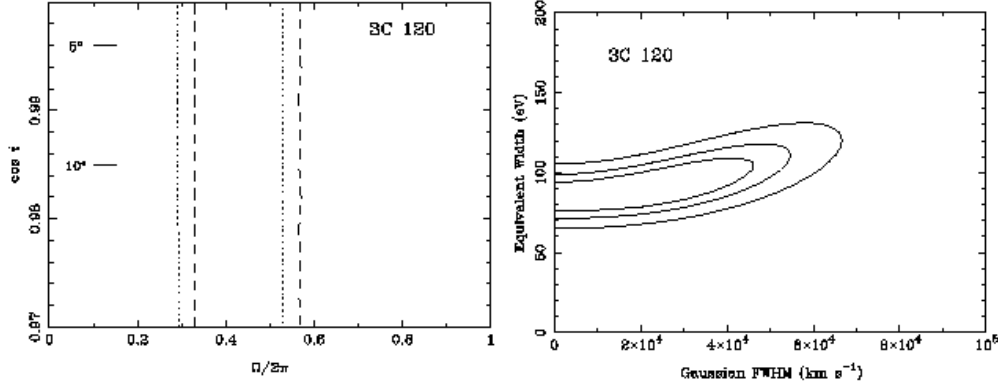


Fig. 2. (a) *Left*: 68, 90, and 99% confidence contours in the width–equivalent width plane showing the properties of the Fe  $K\alpha$  line of 3C 120. The line is obviously unresolved with  $FWHM < 55,00 \text{ km s}^{-1}$ , and an equivalent width of  $90^{+30}_{-20} \text{ eV}$ . (b) *Right*: 90% confidence contours in the disk inclination angle–solid angle plane indicating the allowed strength of the Compton reflection component in 3C 120. The dashed and dotted lines denote the bounds corresponding to different folding energies of the primary X-ray spectrum (300 and 600 keV, respectively). These results are independent of the Fe abundance.

$\gtrsim 20,000 \text{ km s}^{-1}$ , while in NLRGs and RGs it is unresolved. However, it is difficult to study the line profile due to the limited sensitivity of *ASCA* and the fact the line is weak in RL AGNs. Stronger constraints are provided by *RXTE* thanks to its larger collecting area. The Fe  $K\alpha$  line is detected in the BLRGs of the sample (e.g., Figure 2a), with an Equivalent Width of  $EW \lesssim 90 \text{ eV}$ , lower than what was measured by *ASCA* in most Seyferts (Nandra et al. 1997). *RXTE* has been able to detect the Fe  $K\alpha$  line in 3C 111 and Pictor A, where *ASCA* obtained only upper limits of about 100 eV. Unfortunately, because of the poor *RXTE* resolution, the lines are unresolved (Figure 2a).

The wide energy range (2–250 keV) covered by the PCA and HEXTE instruments on *RXTE* is well suited to the study of the Compton reflection in RL AGNs at energies above 10 keV. The strength of this component is parameterized in terms of  $R = \Omega/2\pi$ , i.e., the fraction of solid angle subtended by the reprocessor to the illuminating source. We find (Eracleous, Sambruna, & Mushotzky 1999) that in 2/4 sources (3C 111 and Pictor A) a reflection component is not required to model the data above 10 keV. In 3C 120 and 3C 382, the addition of this component improves significantly the fit, with strength  $R \lesssim 0.4\text{--}0.5$  (see, e.g., Figure 2b). This is lower than what is observed in most Seyferts (Weaver et al. 1998, Lee et al. 1999).

## 4 Interpretation

In the currently accepted accretion scenario for RQ AGNs, X-ray emission is produced in a hot “corona” overlaying and illuminating a standard, Shakura-Sunyaev accretion disk (Haardt et al. 1994). In this picture the reprocessor (disk) subtends a solid angle of  $\Omega = 2\pi$  to the illuminating source, as observed by *Ginga* and *RXTE* in Seyfert galaxies. The Fe  $K\alpha$  line is emitted within a few gravitational radii from the black hole (Fabian et al. 1989), and has a broad red wing. Its equivalent width also depends on the solid angle subtended by the disk to the X-ray source.

In BLRGs we observe weaker reflection components, indicating  $\Omega < 2\pi$ . From this perspective, one possible scenario is the ion torus model (Rees et al. 1982), recently resuscitated in the form of an Advection Dominated Accretion Flow (ADAF; Narayan et al. (1998)). Here the inner parts of the disk (below some transition radius) inflate under the pressure of the ions which are much hotter than the electrons. The latter are responsible for the emitted radiation from radio to IR via synchrotron, bremsstrahlung, and/or inverse Compton emission. The external cold disk would produce the reflection component and the Fe  $K\alpha$  line; both of these features would be weaker than in Seyferts since the disk subtends a solid angle  $\Omega \approx \pi$  to the X-ray source. While this scenario can also accommodate X-ray slopes similar to Seyferts, depending on the size of the transition radius between the inner ADAF and the disk, it does not offer a clear explanation for the high optical and UV luminosities observed in BLRGs.

An alternative scenario was proposed by Woźniak et al. (1998), on the basis of similar results to ours obtained from non-simultaneous, archival *ASCA*, *CGRO/OSSE*, and *Ginga* data. In that scenario the central engines of BLRGs would be occupied by a standard, geometrically thin disk but the bulk of the X-ray continuum would be produced by the inner parts of a relativistic jet. The beamed X-ray component would dilute the strength of both the Fe  $K\alpha$  line and of the reflection component, the latter produced via Thomson scattering in the distant molecular torus. However, our result that RL AGN have similar X-ray slopes to RQ AGNs argues against a beamed component in the X-rays.

In principle, a very good way to discriminate between the two scenarios outlined above is the Fe line profile. The necessary observations will be carried out with *XMM* and *Astro E*. The line will have a distinct profile depending on whether it is produced in the inner regions of a Seyfert-like disk, or at larger distances (external parts of an ADAF or/and the molecular torus). The current and future (e.g., *Constellation X*) X-ray missions also hold the potential to measure precisely the spin of the black hole in RL AGNs, testing models

(Blandford & Znajek 1977, Meier 1999), which posit that RL sources harbor much faster rotating black holes than RQ ones.

## 5 Weak Line Radio Galaxies (WLRGs)

WLRGs were recently identified as powerful lobe-dominated radio galaxies with underluminous [O III] lines and large [O II]/[O III] line ratios (Tadhunter et al. 1998), locating these objects in the LINER/H II-region part of the diagnostic line-ratio diagrams of Filippenko (1996). A proposed explanation is that these systems host a low-luminosity AGN (Tadhunter et al. 1998).

*ASCA* observed and detected six WLRGs. In 5/6 cases, the X-ray spectrum can be decomposed into a hard X-ray component plus a soft thermal component with  $kT \sim 1$  keV. The hard component can be described by either a flat power law,  $\langle \Gamma \rangle = 1.5$  (with individual slopes as flat as  $\Gamma_X = 1.3$ ), or a very hot ( $kT \sim 100$  keV) thermal bremsstrahlung model. The intrinsic luminosity of the hard component is  $L_{2-10 \text{ keV}} \sim 10^{40} - 10^{42} \text{ erg s}^{-1}$ , two orders of magnitude fainter than in the other radio-loud AGNs of the *ASCA* sample. An Fe line with  $EW \sim 250$  eV is marginally detected in two cases.

To understand in more detail the central engines of WLRGs, we studied the case of 3C 270, hosted by the nearby giant elliptical NGC 4261, where *HST* observations provide an estimate of the central black hole mass,  $M_{\text{BH}} = (4.9 \pm 1.0) \times 10^8 M_{\odot}$  (Ferrarese et al. 1996). This implies an Eddington luminosity  $L_{\text{Edd}} \sim (5 - 8) \times 10^{46} \text{ erg s}^{-1}$ . From the radio-to-X-ray spectral energy distribution of 3C 270 (Figure 3a), we estimate a bolometric luminosity of  $L_{\text{Bol}} \sim 2 \times 10^{43} \text{ erg s}^{-1}$ . Thus,  $L_{\text{Bol}}/L_{\text{Edd}} \sim (2 - 4) \times 10^{-4}$ , placing 3C 270 in the ADAF regime (Narayan et al. 1998). It is thus tempting to speculate that WLRGs represent that segment of the population of radio-loud AGN in which the accretion rate is so low that an ADAF is inevitable. In this context, the lack of a strong far-UV ionizing continuum is the cause of the observed underluminous [O III] emission lines.

Interestingly, an Fe line is marginally (90% confidence) detected in 3C 270 between 6.5–7.5 keV with  $EW \sim 250$  eV (Figure 3b). Future observations of this and other WLRGs at higher-sensitivity will allow us to study the line profile and energy, discriminating among possible scenarios for its origin. Particularly intriguing is the possibility that the Fe line originates in the coronal gas in the outer parts of the ADAF (Narayan & Raymond 1999). In this case, soft X-ray lines would be expected as well, whose relative strengths are diagnostics of the size and conditions in the ADAF. Both the Fe and soft X-ray line emission in WLRGs will be well studied by *Chandra* and XMM, which afford an ideal combination of high sensitivity and angular resolution.

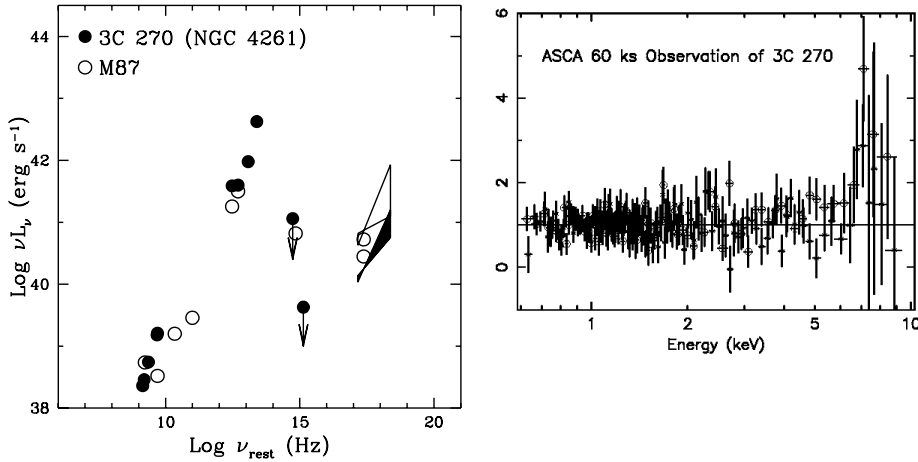


Fig. 3. (a), *Left*: Spectral energy distribution of the Weak Line Radio Galaxy 3C 270 (from *ASCA* and literature data), compared to that of M87. Note the lack of a strong UV continuum. In both cases, the integrated bolometric luminosity is  $10^{-4}$  of the Eddington luminosity. (b), *Right*: The Fe  $K\alpha$  line in the *ASCA* spectrum of 3C 270 (EW  $\sim 250$  eV). A detailed study of the line profile, will have to await observations with XMM.

## 6 Conclusions

We performed an extensive study of the X-ray spectral properties of RL AGNs using *ASCA* and *RXTE*. Our results support a picture where the central engines of RL are systematically different from their RQ counterparts, with RL AGNs having weaker Fe lines and reflection components than RQ ones. The differences also extends to the circumnuclear environments: large columns of cold gas are detected in a fraction of BLRGs and QSRs, while ionized absorption is more typical in Seyfert 1s. Our X-ray results suggest that the origin of the RL/RQ AGN dichotomy must be sought in intrinsic properties of the central engines of these systems, rather than in their larger scale environments (host galaxies/clusters).

We reported the first observations at medium-hard X-rays with *ASCA* of a new subclass of radio galaxies, the WLRGs. There is strong evidence that these systems harbor a low-luminosity AGN in which the accretion flows are advection dominated (e.g., the case study of 3C 270).

The three major X-ray observatories of the next century, *Chandra*, XMM, and Astro E, will have a central role in allowing us to study in detail the Fe line profiles, the nature of the mysterious X-ray absorber, and the structure and geometry of the accretion flow. Future X-ray observations at high sensitivity

and resolution will provide a giant leap forward in our understanding of RL AGNs (comparable to the one *ASCA* already provided for RQ AGNs), opening a new perspective on the origin of the RL/RQ AGN dichotomy.

## Acknowledgements

This work was supported by NASA contract NAS-38252 and NASA grants NAG5-7276 and NAG5-7733.

## References

- Antonucci, R. 1993, ARA&A, 31 473
- Blandford, R. D. & Payne, D. G. 1982, MNRAS, 199, 883
- Blandford, R. D. & Znajek, R. L. 1977, MNRAS, 179, 433
- Cappi, M. et al. 1997, ApJ, 478, 492
- Elvis, M. et al. 1998, ApJ, 492, 91
- Eracleous, M., Sambruna, R. M., & Mushotzky, R. F. 1999, ApJ, *subm.*
- Eracleous, M. & Halpern, J. 1998, ApJ, 505, 577
- Fabian, A. C. et al. 1989, MNRAS, 238, 729
- Ferrarese, L., Ford, H. C., & Jaffe, W. 1996, ApJ, 470, 444
- Filippenko, A. V. 1996, in The Physics of LINERs in View of Recent Observations, ASP Conference Series, vol. 103, eds. M.Eracleous, A.Koratkar, C.Leitherer, & L.Ho, p.17
- George, I. M. & Fabian, A. C. 1991, MNRAS, 249, 352
- George, I. M. et al. 1998, ApJS, 114, 73
- Haardt, F., Maraschi, L., & Ghisellini, G. 1994, ApJ, 432, L95
- Lawson, A.J. et al. 1992, MNRAS, 259, 743
- Lee, J. C. et al. 1999. MNRAS, in press (astro-ph/9907352)
- Meier, D. 1999, these proc. (astro-ph/9908283)
- Nandra, K. & Pounds, K. A. 1994, MNRAS, 268, 405
- Nandra, K. et al. 1997, ApJ, 476, 70

- Narayan, R. & Raymond, J. 1999, ApJ, 515, L69
- Narayan, R. et al. 1998, astro-ph/9803141
- Narayan, R. & Yi, I. 1995, ApJ, 444, 231
- Narayan, R. & Yi, I. 1994, ApJ, 428, L13
- Rees, M.J. et al. 1982, Nature, 295, 17
- Reynolds, C. S. 1997, MNRAS, 286, 513
- Sambruna, R. M., Eracleous, M., & Mushotzky, R. F. 1999, ApJ, in press (astro-ph/9905365)
- Tadhunter, C. N. et al. 1988, MNRAS, 235, 403
- Urry, C. M. & Padovani, P. 1995, PASP, 107, 803
- Weaver, K. A., Krolik, J. H., & Pier, E. A. 1998, ApJ, 498, 213
- Wilkes, B. J. & Elvis, M. 1987, ApJ, 323, 293
- Woźniak, P. et al. 1998, MNRAS, 299, 449